Controlled Reduction with Unactuated Cyclic Variables: Application to 3D Bipedal Walking with Passive Yaw Rotation

Robert D. Gregg and Ludovic Righetti

Abstract—This paper shows that viscous damping can shape momentum conservation laws in a manner that stabilizes yaw rotation and enables steering for underactuated 3D walking. We first show that unactuated cyclic variables can be controlled by passively shaped conservation laws given a stabilizing controller in the actuated coordinates. We then exploit this result to realize controlled geometric reduction with multiple unactuated cyclic variables. We apply this underactuated control strategy to a five-link 3D biped to produce exponentially stable straight-ahead walking and steering in the presence of passive yawing.

I. INTRODUCTION

The realization of humanoid robotic walking in the presence of underactuation is a paramount challenge in control theory. Many researchers have focused on walking without actuation in the lean degree-of-freedom (DOF) of the ankle, but little attention has been given to yaw rotation in the transverse plane [1]. In fact, the human ankle joint provides actuation in the pitch and lean DOFs, but yaw rotation is passive [2]. Body dynamics during walking induce a transverse moment that causes up to 26 degrees of internal/external rotation of the stance leg [3] or pivoting about the ground contact point, which humans exploit in their turning strategies [4].

In order to passively control yaw in humanoid robots, lessons might be learned from the design of passive prosthetic legs. Rigid prostheses often cause painful shear forces on the skin of the residual limb, so many prosthetic legs have transverse rotation adapters that alleviate shear forces by providing a passive yaw DOF to absorb transverse moments [5]. However, these prosthetic adapters are made with a wide range of stiffness and viscosity properties, which in some cases increase the yaw range-of-motion compared to able-bodied walking [3]. The effect of this passive DOF on gait stability, especially during turning motions, has yet to be addressed.

Recent work considers the stability of bipedal robots with unactuated roll, pitch, and yaw about point feet [6]. This rigorous control approach, known as hybrid zero dynamics (cf. [7]), uses the actuated DOFs to linearize output dynamics associated with virtual constraints, which characterize optimized joint patterns. However, we are interested in the control of passive yaw rotation in human-like legs with ankle actuation.

Using actuated roll, pitch, and yaw at the ankle, controlled reduction (cf. [8]–[11]) exploits momentum conservation laws to create zero dynamics equivalent to known *passively* stable bipeds (i.e., gravity-powered walking down slopes [12]). Rather than designing gaits via optimization, this approach exploits the existence of passive limit cycles in the sagittal plane as a sufficient condition for a controller that stabilizes 3D limit cycles [13]. Straight-ahead and steering gaits for a 3D biped with full actuation are simulated in [9], enabling motion planning applications for fast and efficient asymptotically stable walkers [14]. However, this body of work has not shown how walking and steering can be achieved with underactuation.

This paper shows that viscous damping can shape momentum conservation laws in a manner that stabilizes yaw rotation and enables steering for underactuated 3D walking. We show in Section II that unactuated cyclic variables can be controlled by passively shaped conservation laws given a stabilizing controller in the actuated coordinates. This enables controlled reduction from [11] to be realized with multiple unactuated cyclic variables in Section III, generalizing the initial work [15] that considered one unactuated variable. We apply the controller to a five-link 3D biped with passive yaw rotation in Section IV, going beyond [15] by realizing steering motion and considering model uncertainty. We conclude in Section V.

II. PASSIVELY SHAPED CONSERVATION LAWS

We consider the class of n-DOF mechanical systems with configuration space $\mathcal{Q} = \mathbb{R}^n$, where the state $(q, \dot{q})$ in tangent bundle $T\mathcal{Q} \cong \mathbb{R}^{2n}$ consists of configuration $q \in \mathcal{Q}$ and joint velocities $\dot{q} \in \mathbb{R}^n$. The dynamics are derived from the Lagrangian $\mathcal{L} : T\mathcal{Q} \to \mathbb{R}$, given in coordinates by $\mathcal{L}(q, \dot{q}) = \frac{1}{2}\dot{q}^T M(q)\dot{q} - \mathcal{V}(q)$, where $\mathcal{V}(q)$ is the potential energy and $n \times n$ symmetric, positive-definite $M(q)$ is the inertia matrix. Integral curves satisfy the *Euler-Lagrange* equations

$$\frac{d}{dt}\nabla_{\dot{q}}\mathcal{L} - \nabla_q \mathcal{L} = \tau, \tag{1}$$

where $\tau \in \mathbb{R}^n$ contains the external joint torques. This second-order system of ordinary differential equations gives the dynamics for the actuated mechanism in phase space $T\mathcal{Q}$:

$$M(q)\ddot{q} + C(q, \dot{q})\dot{q} + N(q) = Bu, \tag{2}$$

where $n \times n$-matrix $C(q, \dot{q})$ contains the Coriolis/centrifugal terms, vector $N(q) = \nabla_q \mathcal{V}(q)$ contains the potential torques, and $n \times m$-matrix B (full row rank) maps actuator input vector $u \in \mathbb{R}^m$ to joint torques $\tau = Bu \in \mathbb{R}^n$ for $m \leq n$.

Lagrangian symmetry implies a *conservation law* by Noether's theorem [16], i.e., a physical quantity of the system is conserved by the dynamics. We are interested in conservation laws that can be expressed as constraints of the form

$$J_c(q)\dot{q} = b(q), \tag{3}$$

where constraint Jacobian $J_c \in \mathbb{R}^{k \times n}$ has rank $k < n$. Given such a conservation law, the system dynamics are restricted to the invariant level-set

$$\mathcal{Z} = \{(q, \dot{q}) \mid J_c(q)\dot{q} - b(q) = 0\}. \qquad (4)$$

Definition 1: Let Lagrangian $\mathcal{L}$ be defined in the coordinates of configuration space $\mathcal{Q} = \mathbb{G} \times S$, where $\mathbb{G} = \mathbb{R}^k$ is known as the *symmetry group* and $S = \mathbb{R}^{n-k}$ as the *shape space*. Then, *cyclic* variables $q_1 \in \mathbb{G}$ are such that $\nabla_{q_1} \mathcal{L} = 0$.

When cyclic variables are free from external forces ($\tau_1 = 0$), equation (1) implies that the generalized momenta $p_1 = \nabla_{\dot{q}_1} \mathcal{L}$ conjugate to the cyclic coordinates are constant. The dynamics then evolve on the invariant level-set (4) of these conserved momentum quantities, where $J_c = [I_{k \times k} \quad 0_{k \times n-k}]M$ and $b(q) = \mu$ for some constant vector μ.

Many systems have an unactuated cyclic variable and actuated shape variables, for which a stabilizing controller exists when the momentum conservation law is broken with a rotary spring in the cyclic coordinate [17]. Since springs cannot always be physically realized in cyclic coordinates (e.g., at ground contact points), we will instead use *viscous damping* (e.g., from friction) to shape the existing conservation law and subsequently control multiple cyclic variables. In particular, we want the shaped conservation law to control the cyclic coordinates $q_1 \in \mathbb{G}$ to periodic orbits given periodicity in the shape coordinates $q_s \in S$, where $q = (q_1^T, q_s^T)^T$.

Lemma 1: Let q_1 be a vector of cyclic coordinates in system (1). Then passive joint-velocity feedback $\tau_1 = -K_1 \dot{q}_1$, for diagonal and positive-definite $K_1 \in \mathbb{R}^{k \times k}$, implies the *functional* conservation law

$$J_c(q)\dot{q} = -K_1(q_1 - \bar{q}_1) \qquad (5)$$

for some constant vector $\bar{q}_1$ satisfying initial boundary condition $p_1(t_0) = -K_1(q_1(t_0) - \bar{q}_1)$.

Proof: Given $\nabla_{q_1} \mathcal{L} = 0$, plugging τ_1 into (1) implies $\dot{p}_1 = -K_1 \dot{q}_1$. Momentum $p_1 = \nabla_{\dot{q}_1} \mathcal{L}$ is no longer conserved as a constant but rather as a function by the fundamental theorem of calculus: $p_1(t) = p_1(t_0) - \int_{t_0}^{t} K_1 \dot{q}_1(\tau)d\tau = p_1(t_0) - K_1(q_1(t) - q_1(t_0))$. Given the initial boundary condition above, we have $p_1(t) = -K_1(q_1(t) - \bar{q}_1)$ for all $t \geq t_0$. ∎

Remark 1: Every initial condition has an associated conservation law, so we have rendered invariant infinitely-many submanifolds $\mathcal{Z}_{\bar{q}_1}$ as in (4), each parameterized by $\bar{q}_1$. This continuously parameterized submanifold is known as a *foliation* of manifold $T\mathcal{Q}$.

Remark 2: We see the benefit of functional conservation law (5) by rewriting it in the form

$$\dot{q}_1 = -M_1^{-1}(q_s)[K_1(q_1 - \bar{q}_1) + M_{1,s}(q_s)\dot{q}_s], \qquad (6)$$

where M_1 is the $k \times k$ upper-left submatrix of M and $M_{1,s}$ is the $k \times n - k$ upper-right submatrix. Equation (6) is a homogeneous first-order linear system in q_1 with time-varying coefficients based on trajectories $q_s(t), \dot{q}_s(t)$. The diagonal blocks of inertia matrix M are positive definite, implying that $M_1^{-1} K_1$ is also positive definite. System (6) then has negative-gain linearity in q_1, by which we can prove the existence of a

unique T-periodic orbit $(q_1^*(t), \dot{q}_1^*(t))$ in a neighborhood about $\bar{q}_1$ given the existence of a T-periodic orbit $(q_s^*(t), \dot{q}_s^*(t))$. Asymptotic convergence in the shape variables similarly implies asymptotic convergence in the cyclic variables [18].

Therefore, given a stabilizing feedback controller for the shape variables, Lemma 1 implies that viscous damping—whether from a mechanical damper or environmental friction—controls the cyclic coordinates q_1 to a neighborhood determined by the initial conditions and the shape variable trajectory. (Lemma 1 can also be generalized to consider nonlinear damping [19].) This result is applicable to any underactuated control strategy that stabilizes the shape variables (e.g., hybrid zero dynamics for a biped with point feet [6], [7]), but we will use it for the second contribution of this paper: achieving controlled reduction with underactuation.

III. UNDERACTUATED CONTROLLED REDUCTION

In this section we will use Lemma 1 to realize the controlled version of Routhian reduction—known as *functional* Routhian reduction [8]–[11], [13]—with unactuated cyclic variables.

Recursively Cyclic Variables. In mechanical systems often only the world coordinates are cyclic, e.g., position and orientation of the stance foot. However, inertia matrices of kinematic chains have a special structure with *recursively cyclic* variables [8], [9]. To handle vectors of cyclic variables, we generalize this property to *block* recursively cyclic variables:

Lemma 2: For any n-DOF serial kinematic chain there exist an integer $k_1 \geq 1$ and (local) generalized coordinates $q = (q_1^T, q_2^T)^T$, $\dim q_1 = k_1$, such that the $n \times n$ inertia matrix M does not depend on q_1. Additionally, the lower-right $n - k_1 \times n - k_1$ submatrix of M is the inertia matrix of the $(n - k_1)$-DOF serial kinematic chain corresponding to the original n-DOF kinematic chain with coordinates q_1 fixed.

Proposition 1: For any n-DOF serial kinematic chain there exist integers $k_1, \ldots, k_j \geq 1$, $\sum_{i \in \{1,\ldots,j\}} k_i = n$, and (local) generalized coordinates $q = (q_1^T, \ldots, q_j^T)^T$, $\dim q_i = k_i$ for all $i \in \{1, \ldots, j\}$, such that the inertia matrix M is independent of q_1 and the lower-right $(n - k_1 - \ldots - k_i) \times (n - k_1 - \ldots - k_i)$ submatrix of M is independent of q_{i+1} for all $i \in \{1, \ldots, j - 1\}$.

This recursively cyclic structure holds down to a constant submatrix. Lemma 2 is proven by the same arguments in [8] (in which $k_i = 1$), and Proposition 1 follows from Lemma 2 by induction. Note that this result is easily extended to branched kinematic chains as in [9].

We can extend the functional conservation law (5) to the case of block recursively cyclic variables. The configuration is first partitioned into $q = (q_c^T, q_r^T)^T$, where block recursively cyclic variables are contained in the *constrained* coordinates $q_c = (q_1^T, q_2^T, \ldots)^T \in \mathbb{R}^k$, $k = \sum k_i$, and the remaining variables (to be decoupled by the controlled reduction) are in the *reduced* coordinates $q_r \in \mathbb{R}^{n-k}$. Since we have defined global coordinates here, we must ensure the local coordinates from Proposition 1 hold over the relevant domain for a given dynamical system. In the case of bipedal locomotion, joints have limited range of motion and this condition is ensured.

We exploit the block recursively cyclic property by considering the momentum $\hat{p} := \hat{M}\dot{q}$, where matrix $\hat{M}$ is defined by upper-triangular blocks from M:

$$\hat{M}(q) = \begin{pmatrix} \hat{M}_c(q_c, q_r) & M_{c,r}(q_c, q_r) \\ 0 & M_r(q_r) \end{pmatrix}, \quad (7)$$

$$\hat{M}_c(q) = \begin{pmatrix} M_1(q_2, q_3, \ldots) & * & * \\ 0 & M_2(q_3, \ldots) & * \\ 0 & 0 & \ddots \end{pmatrix},$$

where $M_{c,r} \in \mathbb{R}^{k \times n-k}$ and $M_r \in \mathbb{R}^{n-k \times n-k}$ are respectively the top-right and bottom-right submatrices in M, and $\hat{M}_c \in \mathbb{R}^{k \times k}$ is the block upper-triangular part of the top-left submatrix in M (asterisk indicates off-diagonal term from M). The first k momentum terms are then given by $\hat{p}_c = [\hat{M}_c \quad M_{c,r}]\dot{q}$. To control coordinates q_c to neighborhoods around set-points $\bar{q}_c \in \mathbb{R}^k$, we will constrain these momenta to

$$\hat{p}_c = -K(q_c - \bar{q}_c) \quad (8)$$
$$\iff \dot{q}_c = -\hat{M}_c^{-1}\left[K(q_c - \bar{q}_c) + M_{c,r}\dot{q}_r\right],$$

where gain matrix $K \in \mathbb{R}^{k \times k}$ is constant, diagonal, and positive-definite. These constraints define a smooth, invariant, $(2n - k)$-dimensional submanifold $\mathcal{Z}_{\bar{q}_c}$ as in (4), where $J_c = [\hat{M}_c \quad M_{c,r}]$ and $b = -K(q_c - \bar{q}_c)$ is continuously parameterized by $\bar{q}_c$. Note by definition $\hat{p}_1 = p_1$, so constraint (8) includes the shaped conservation law (5) provided by passive damping in Lemma 1.

The recursively cyclic and upper-triangular structure of $\hat{M}$ implies that scaling matrices $\hat{M}_c^{-1}K$ and $\hat{M}_c^{-1}M_{c,r}$ have no dependence on coordinates $q_{1,\ldots,i}$ in row i, for $i \in 1, \ldots, k$. The argument from Remark 2 can then be invoked to prove convergence to a periodic orbit in the constrained coordinates given convergence in the reduced coordinates. These constraints will decompose the control problem into upper-triangular form, allowing us to construct limit cycles for locomotion in a manner analogous to forwarding/backstepping [20].

Nullspace Projection. Although controlled reduction was originally derived with Lagrangian shaping [8]–[10], [13], we use inverse dynamics to insert joint accelerations that directly enforce the desired constraints and decouple the reduced coordinates. We will show that this formulation from [11] can be achieved with unactuated cyclic variables. Constraint Jacobian $J_c = [\hat{M}_c \quad M_{c,r}]$ maps joint velocities to momenta in first-order constraint (3), but this Jacobian can also map joint accelerations to torques. We take the time-derivative of (3) to obtain the second-order constraint

$$J_c\ddot{q} = -\dot{J}_c\dot{q} + \dot{b}, \quad (9)$$

where $\dot{J}_c = [\dot{\hat{M}}_c \quad \dot{M}_{c,r}]$ and $\dot{b} = -K\dot{q}_c$. This second-order constraint is independent of set-point $\bar{q}_c$ and renders invariant infinitely-many first-order manifolds $\mathcal{Z}_{\bar{q}_c}$ in a foliation of $T\mathcal{Q}$.

We now design accelerations $\ddot{q}_d \in \mathbb{R}^n$ that enforce (9) and follow the reference $\ddot{q}_{\text{ref}} = (\ddot{q}_{c_d}^T, \ddot{q}_{r_d}^T)^T \in \mathbb{R}^n$ within the constraint nullspace. Motivated by hierarchical operational space control [21], constraint enforcement is the primary task and tracking $\ddot{q}_{\text{ref}}$ is a secondary task that complies with the

primary. Solutions for this desired acceleration are given by

$$\ddot{q}_d = J_c^-(-\dot{J}_c\dot{q} - K\dot{q}_c) + (I - J_c^- J_c)\ddot{q}_{\text{ref}}, \quad (10)$$

where $J_c^- \in \mathbb{R}^{n \times k}$ denotes any generalized inverse of J_c (i.e., a matrix such that $J_c J_c^- J_c = J_c$).

Since J_c is full row rank, we can choose an inverse of the form $J_c^- = W J_c^T (J_c W J_c^T)^{-1}$, where $W \in \mathbb{R}^{n \times n}$ is a positive-definite weight matrix that manipulates how accelerations $\ddot{q}_{\text{ref}}$ are projected into the nullspace of the constraints. We choose $W = \hat{M}^{-T}$ so that $J_c^- = [\hat{M}_c^{-T} \quad 0]^T$ and its nullspace projector $(I - J_c^- J_c)$ triangularize the dynamics:

$$\ddot{q}_d = \begin{pmatrix} -\hat{M}_c^{-1}(\dot{J}_c\dot{q} + K\dot{q}_c + M_{c,r}\ddot{q}_{r_d}) + [0_{1 \times k_1}, v^T]^T \\ \ddot{q}_{r_d} \end{pmatrix}, \quad (11)$$

where we have added an auxiliary input $v \in \mathbb{R}^{k-k_1}$ to be defined later. The nullspace projector removes any dependence on $\ddot{q}_{c_d}$—the first k coordinates instead evolve according to the constraints—leaving command over the reference $\ddot{q}_{r_d}$ in the decoupled reduced partition. This term also appears in the constrained dynamics, which synchronizes the partitions (so all planes-of-motion of a 3D biped have the same orbital period).

Starting with the case of full actuation, the inverse dynamics controller that provides joint accelerations (11) in system (1) is given by $\tau_{\text{full}}(q, \dot{q}) := M\ddot{q}_d + C\dot{q} + N$.

Underactuation. Although second-order constraint (9) is always enforced by τ_{full}, initial conditions determine one of infinitely-many first-order constraints (3). System (11) possesses a symmetry with respect to set-points of the constrained coordinates. This may be desirable in some DOFs, e.g., biped dynamics should be invariant with respect to global heading on a flat surface. We can achieve this foliation of $T\mathcal{Q}$ even if the cyclic coordinates $q_1 \in \mathbb{R}^{k_1}$ are unactuated, *provided they are subject to viscous damping from passive forces.*

Proposition 2: Let $q_1 \in \mathbb{R}^{k_1}$ be the cyclic coordinate vector for $k_1 \geq 1$. Then the first k_1 terms of control law τ_{full} are equivalent to viscous damping, i.e., $S_n^\top \tau_{\text{full}}(q, \dot{q}) = -K_1\dot{q}_1$, where $S_n^\top = [I_{k_1 \times k_1} \quad 0_{k_1 \times n-k_1}]$ is a selector matrix and $K_1 \in \mathbb{R}^{k_1 \times k_1}$ is the top-left (diagonal) submatrix of K.

Proof: To begin, note that $S_n^\top M = S_k^\top [M_c \quad M_{c,r}]$ with $S_k^\top = [I_{k_1 \times k_1} \quad 0_{k_1 \times k-k_1}]$, and the block recursively cyclic structure of M_c provides $S_k^\top M_c \hat{M}_c^{-1} = S_k^\top$. Plugging (11) into τ_{full}, we find that $S_n^\top M\ddot{q}_d = -S_k^\top \dot{J}_c\dot{q} - K_1\dot{q}_1$. The proof is completed by noting that $\nabla_{q_1}\mathcal{L} = 0$ implies $S_n^\top N = \nabla_{q_1}\mathcal{V} = 0$, and $S_n^\top C\dot{q} - S_k^\top \dot{J}_c\dot{q} = 0$ by definition of Coriolis matrix C:

$$c_{ij} = \frac{1}{2}\dot{m}_{ij} + \frac{1}{2}\sum_{h=1}^n \left(\frac{\partial m_{ih}}{\partial q_j} - \frac{\partial m_{jh}}{\partial q_i}\right)\dot{q}_h,$$

where i, j, h are indices of matrices C and M, and $\partial m_{jh}/\partial q_i = 0$ for $i = 1, \ldots, k_1$. ∎

Hence, the first control terms—corresponding to the purely cyclic coordinates—can be provided by passive forces instead of actuation. These terms enforce the second-order constraint with respect to coordinates q_1 by Lemma 1, and the remaining control terms in τ_{full} enforce the remaining $k - k_1$ second-order constraints. Letting $B = [0_{n-k_1 \times k_1} \quad I_{n-k_1 \times n-k_1}]^T$ in system (2), the underactuated version of the controller is then

$$u_{\text{und}}(q, \dot{q}) := B^T \tau_{\text{full}}(q, \dot{q}). \quad (12)$$
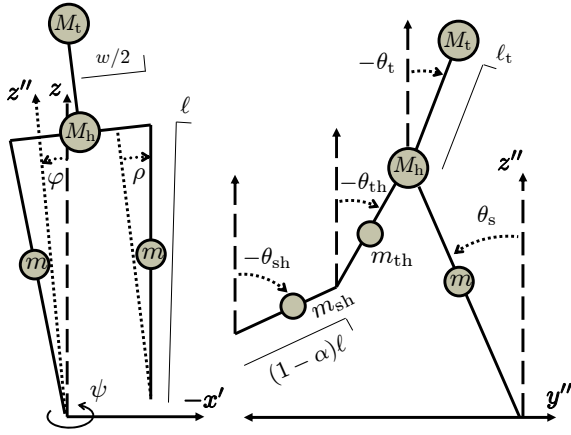
Fig. 1. Diagram of 3D biped's frontal (left) and sagittal (right) planes.

This control law depends on the passive damping coefficients of K_1, but we will see in the biped application of Section IV that (12) is quite robust to uncertainty in this coefficient.

For $v = 0$ any solution trajectory of (2) under (12) belongs to a submanifold $\mathcal{Z}_{\bar{q}_c}$ with respect to a specific vector $\bar{q}_c$, which is determined by the initial conditions as in Lemma 1. However, we can use auxiliary input v to control the $k - k_1$ actuated constrained coordinates to desired set-points. We wish to render exponentially attractive the surface $\mathcal{Z}_{k-k_1}$ defined by the last $k - k_1$ first-order constraints of $\mathcal{Z}_{\bar{q}_c}$, where $\mathcal{Z}_{\bar{q}_c} \subset \mathcal{Z}_{k-k_1}$. This is equivalent to zeroing $k - k_1$ outputs $y := \mathrm{S}^\perp (J_c \dot{q} - b)$ with selector matrix $\mathrm{S}^\perp = [0_{k-k_1 \times k_1} \quad I_{k-k_1 \times k-k_1}]$, so we feedback linearize the associated output dynamics into the exponentially stable system $\dot{y} = -Ly$ for some positive-definite matrix $L \in \mathbb{R}^{k-k_1 \times k-k_1}$. Plugging (11) into the expression for $\dot{y}$, we solve for the linearizing control law:

$$v_{\mathrm{linz}}(q, \dot{q}) \;\; = \;\; -\mathrm{S}^\perp \hat{M}_c^{-1} \mathrm{S}^{\perp^T} Ly. \qquad (13)$$

Because y enters linearly into (13), this subcontroller is zero when restricted to the constraint surface $\mathcal{Z}_{k-k_1}$, i.e., when $y = 0$. We now apply control (12) with $v = v_{\mathrm{linz}}(q, \dot{q})$ to a biped.

IV. APPLICATION TO A 3D BIPED

The 3D biped model in Fig. 1 has two continuous phases during a step cycle: a knee-swing phase with six DOFs and a knee-lock phase with five DOFs. The knee of the stance leg remains locked during each step. We assume the stance foot remains flat on the ground with sufficient Coulomb friction to prevent slipping. This model has one cyclic coordinate (the yaw DOF) subject to damping with a known viscosity, which can be physically realized by a rotary damper (e.g., a transverse rotation adapter [5]) at the ankle joint. The human analog would be soft and hard tissues in the stance leg, which internally/externally rotates during walking [2].

Biped Model. The biped coordinates are $q = (\psi, \varphi, \theta^T)^T$, where yaw/heading ψ and roll/lean φ are defined at the stance ankle, and vector $\theta = (\theta_s, \theta_t, \theta_{th}, \theta_{sh})^T$ contains the sagittal-plane (pitch) variables for the stance leg, torso, swing thigh, and swing shank, respectively. Knee-lock phase provides $\theta_{th} \equiv \theta_{sh}$. The hip abduction/adduction joints in Fig. 1 are fixed to a constant ρ to simplify the model.

The system state $x = (q^T, \dot{q}^T)^T$ is in domain D, defined as the subset of $T\mathcal{Q}$ such that the swing foot height is non-negative. We assume that both knee-strike and ground-strike impact events are instantaneous and perfectly plastic, resulting in transitions between six and five DOF dynamics (called phases) according to a hybrid system $\mathcal{H}$ (see [15] for details). The model terms of (2) for each phase are provided in supplemental *Mathematica* files. The ground-strike guard G_g is defined as the subset of D where the swing foot height is zero, and its reset map $\Delta_g(x)$ is computed as in [7]. The knee-strike guard G_k is the subset of D where $\theta_{th} - \theta_{sh} = 0$, and its reset map $\Delta_k(x)$ is computed as in [22]. The dynamics are mirrored between each leg's stance phase.

We partition the configuration into constrained coordinates $q_c = (\psi, \varphi)^T$ and reduced coordinates $q_r = \theta$, i.e., $k = 2$. Yaw is the first DOF in the kinematic chain and is defined about the gravity vector on a flat surface, implying that $q_1 = \psi$ is a cyclic variable ($k_1 = 1$). We adopt yaw viscosity $K_1 = K_\psi = 0.5$ and the parameters in Table I for all phases in $\mathcal{H}$. Controller (12) enters into coordinates φ, θ with actuator saturation at U_{max}. Lean $q_2 = \varphi$ is the only constrained coordinate that is controlled by output linearization to a specific set-point, $\bar{\varphi} = 0$, corresponding to upright.

We build pseudo-passive walking gaits by closing an outer feedback loop that inserts sagittal-plane dynamics into the unconstrained accelerations of (11):

$$\ddot{\theta}_d = M_\theta^{-1}(\theta)([0, v_{pd}, 0]^T - C_\theta(\theta, \dot{\theta})\dot{\theta} - N_\theta(\theta + \beta)), \quad (14)$$

which both keeps the torso upright with $v_{pd} := -k_p \theta_t - k_d \dot{\theta}_t$ and virtually rotates the gravity vector to mimic downhill dynamics (slope angle β) on flat ground [12]. This slope-changing "controlled symmetry" exploits passive limit cycles to stabilize the reduced subsystem.

Results. We show the existence and exponential stability of hybrid limit cycles by the *method of Poincaré sections* [7]. Recall that system $\mathcal{H}$ under (12) is invariant with respect to heading, implying that no isolated orbits exist in the given coordinate system. We therefore analyze the hybrid system *modulo* yaw, for which a hybrid limit cycle may exist with respect to the change in heading over the gait cycle, i.e., a steering angle $s \in \mathbb{R}$. Defining a return map $P : G_g \to G_g$ between ground-strike events, we will find fixed points $x^*(s) = P^2(x^*(s)) - [s, 0]^T$. The return map does not depend on the global heading, so $x^*(s) + [s + \delta, 0]^T = P^2(x^*(s) + [\delta, 0]^T)$ for all $\delta \in \mathbb{R}$. We can numerically linearize the Poincaré map P^2 about fixed points to show that all eigenvalues are within the unit circle, confirming exponential stability of the discrete system (and thus the hybrid system [7]) for a net amount of yaw rotation rather than a global heading.

1) Straight-ahead gait: We find an exponentially stable fixed point $x^*(0) = P^2(x^*(0))$ for zero net yaw. We see in Fig. 2 (top-center) that the discontinuous impact events violate the desired first-order constraint, i.e., submanifold $\mathcal{Z}_{\bar{q}_c}$ is not *hybrid* invariant. Since the second-order constraint (9) is always enforced under control (12), the post-impact state is contained in the submanifold of a different set-point $\bar{q}_c$. Subcontroller (13) corrects the error in lean output y_φ shortly

TABLE I
MODEL PARAMETERS AND FIXED POINTS FOR FIVE-LINK 3D BIPED

Model	:	$M_\mathrm{t} = 15$ kg, $\ell_\mathrm{t} = 0.55$ m, $M_\mathrm{h} = 10$ kg, $m = 5$ kg, $m_\mathrm{th} = 0.7 \cdot m$, $m_\mathrm{sh} = 0.3 \cdot m$, $\ell = 1$ m, $\rho = 0.0564$ rad,
		$\alpha = 0.5, w = 0.2$ m, $K_\psi = 0.5$, $K_\varphi = 30$, $L = 55$, $k_\mathrm{p} = 700$, $k_\mathrm{d} = 300$, $\beta = 0.06$ rad, $U_\mathrm{max} = 40$ Nm
$x^*(0)$	$\approx$	$(0, -0.0020, -0.3084, -0.0534, 0.3089, 0.3089, -0.1653, 0.0201, -1.5743, 0.1941, -1.5516, -1.5516)^T$
$x^*(\bar{s})$	$\approx$	$(0, 0.0020, -0.3055, -0.0632, 0.3049, 0.3049, -0.1265, 0.0222, -1.5657, 0.2161, -1.8355, -1.8355)^T$

after each impulse so that the desired set-point ($\bar{\varphi} = 0$) holds for enough of the step period to keep the biped upright. The yaw output y_ψ is not corrected so it is piecewise constant.

Recall that a constant value of y_ψ does not imply that yaw is constant, but rather that the biped rotates toward some heading $\bar{\psi}$ parameterizing the first-order constraint of that continuous phase. The change in y_ψ across double-support transitions is equal and opposite every step, resulting in a constant net heading over the two-step gait cycle. Jumps in y_ψ cause directional changes in the yaw trajectory of Fig. 2 (middle-left) that qualitatively resemble the internal/external rotation of the tibia during human walking [2, Fig. 1-15].

2) Damping: We next examine the effect of viscosity K_ψ, which enters into control (12). Decreasing the coefficient from $K_\psi = 1$, we see in Fig. 3 (top) that instability ensues for coefficients smaller than $K_\psi = 0.4$, which demonstrates that the yaw DOF requires a certain amount of damping for gait stability. We find that both the maximum eigenvalue modulus and the yaw range-of-motion increase as viscosity decreases.

3) Steering: We now construct steering gaits that can be used for motion planning [14]. Although we do not have direct control over heading set-point $\bar{\psi}$, a desired lean angle $\bar{\varphi}$ can be forced by subcontroller (13). This angle can be chosen to induce a yaw moment, effectively changing the constraint set-point $\bar{\psi}$ by leaning into the direction of this desired heading.

The outer leg should travel a greater distance than the inner leg of a turn, so we use an event-based controller that sets $\bar{\varphi}$ to zero during outer leg stance and a non-zero value $\bar{\varphi}_\mathrm{in}$ during inner leg stance. For a range of $\bar{\varphi}_\mathrm{in}$ values we observe convergence to fixed points modulo yaw, which are confirmed locally exponentially stable in Fig. 3 (bottom). We show the turning gait for $\bar{\varphi}_\mathrm{in} = 0.007$ in Fig. 4, which corresponds to an exponentially stable fixed point $x^*(\bar{s}) = P^2(x^*(\bar{s})) - [\bar{s}, 0]^T$ with steering angle $\bar{s} = s(\bar{\varphi}_\mathrm{in}) = 0.1498$ rad.

4) Contact constraints: In order to validate the feasibility of our contact assumptions, we need to show that the center of pressure (COP)—the point at which the ground reaction force (GRF) is exerted—stays within a reasonably sized foot. Additionally, the GRF vector $[F_1, F_2, F_3]^T$ must satisfy two conditions: the vertical component is strictly positive, i.e., $F_3(t) > 0$ for all t, and the vector remains within the friction cone, i.e., $\mathrm{norm}([F_1(t), F_2(t)])/|F_3(t)| < \eta$ for all t, with a moderate Coulomb friction coefficient of $\eta = 0.45$.

During straight-ahead walking the COP moves in front of the ankle up to 11.3 cm and laterally from the ankle up to 7.9 cm (i.e., away from the body). For our turning gait the COP moves 11.6 cm in front of the ankle and 11.1 cm laterally from the ankle. This implies that a 11.6 cm by 11.1 cm foot is sufficiently large to remain flat. This length is well within human ranges (the average male foot is 25.8 cm long [23]),

but the width is somewhat disproportionate. Wide feet are common in humanoid robots to date (e.g., NAO and ASIMO), but our foot width could possibly be decreased by optimizing parameters, e.g., lowering the lean gain L.

We verify the remaining two GRF conditions (Fig. 2, bottom-left) using the procedure in [24]. Note that the GRF only approaches the boundary of the friction cone at the end of the stance phase, which is characteristic of the foot beginning to lift off at the double-support transition [2].

5) Efficiency: Integrating $\dot{q}^T B u$ to obtain the net work per step, we find that the *mechanical* cost of transport (work done per unit weight-distance) for both gaits is 0.058, which compares with passive dynamic robots such as the Cornell biped at 0.055 [25]. By choosing momentum constraints based on symmetries and reinserting the original planar dynamics, our inverse dynamics approach retains the efficiency that is characteristic of passive dynamic walking.

6) Model uncertainty: Virtual constraints are often implemented in practice using high-gain PD control instead of the exact model-dependent controller [7], but recent results on the bipedal robot MABEL show that model-based output linearization is in fact feasible [26]. A common consequence of modeling errors is stable but asymmetric walking gaits.

In our virtual constraint formulation, control law (12) computes the desired accelerations (11) by inverting the upper-triangular $\hat{M}_c$, which is 2×2 in our application, rather than the full 6×6 inertia matrix M as in Lagrangian-shaping approaches [8], [13]. This will amplify fewer of the modeling errors in a hardware implementation. To demonstrate this principle, we perform simulations with model uncertainty in the control law computation. We introduce 5% errors in all mass parameters and w, which results in stable walking that repeats every 8 steps (Fig. 2, bottom-right). Recalling that controller (12) depends on yaw damping coefficient K_ψ to determine the desired submanifold, we are also able to generate stable walking with coefficient errors in excess of 35%. This demonstrates some robustness to model uncertainty.

V. CONCLUSIONS

These results show that control authority over steering can be achieved using passive damping (e.g., from tendons or transverse rotation adapters) to harness coupling with the body through momentum conservation laws. We exploited these conservation laws to realize controlled geometric reduction with underactuation. We then produced exponentially stable walking and steering for a five-link 3D biped, despite passive yawing and actuator saturation at the other DOFs.

This theoretically rigorous control law is promising for implementation by providing robustness to model uncertainty. This work also suggests that prosthetic rotation adapters,
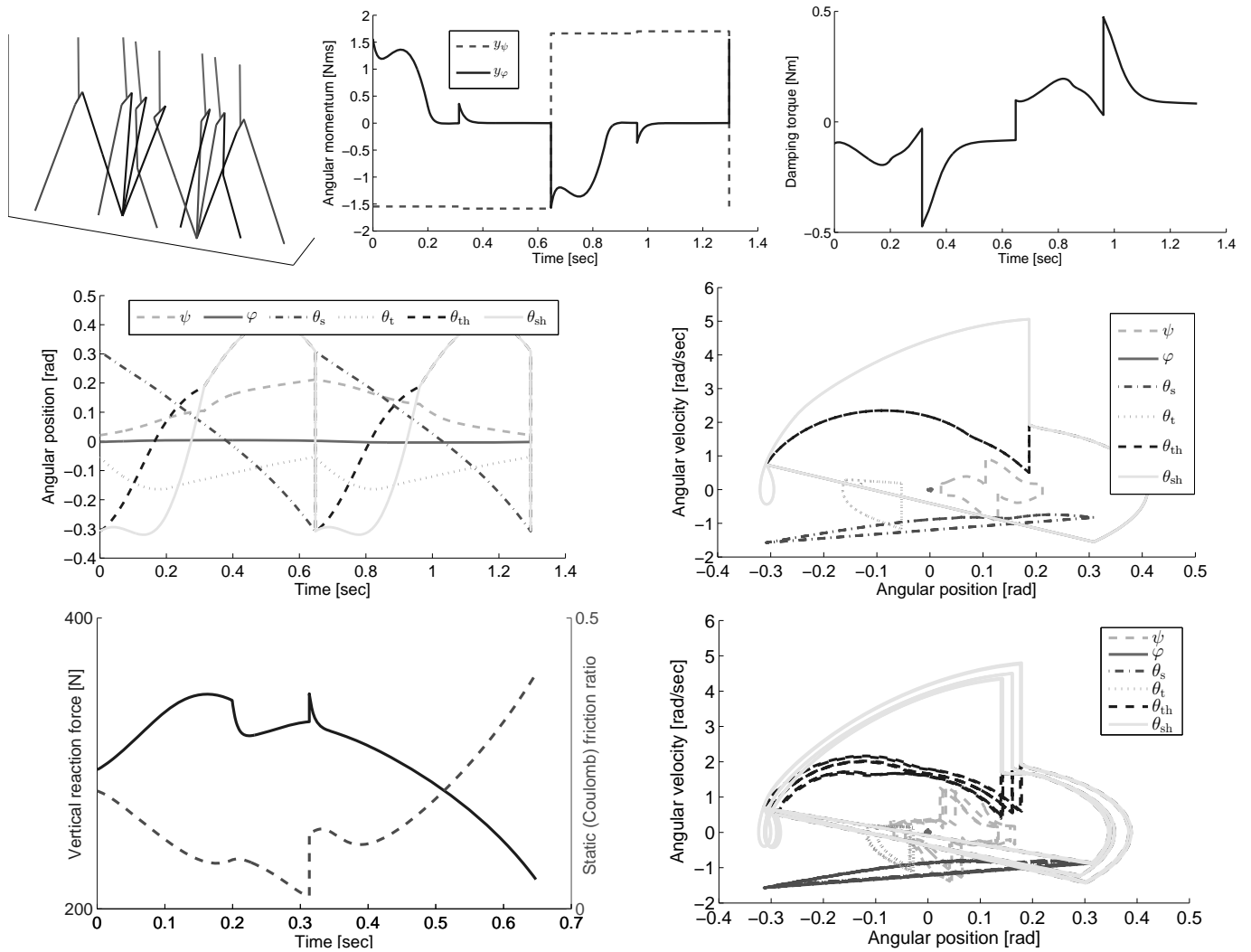
Fig. 2. Straight-ahead gait animation (top-left), outputs $y_\psi = [1 \quad 0]J_c\dot{q} + K_\psi\psi$ and $y_\varphi = [0 \quad 1 \quad 0]J_c\dot{q} + K_\varphi\varphi$ (top-center), yaw damping torque (top-right), joint trajectories (middle-left), and phase portrait (middle-right) over two steps. A movie is available at: http://vimeo.com/20956363. Bottom-left: Vertical GRF (solid, left axis) and GRF friction ratio (dashed, right axis) over one step. Bottom-right: Phase portrait of 8 steps under model uncertainty.
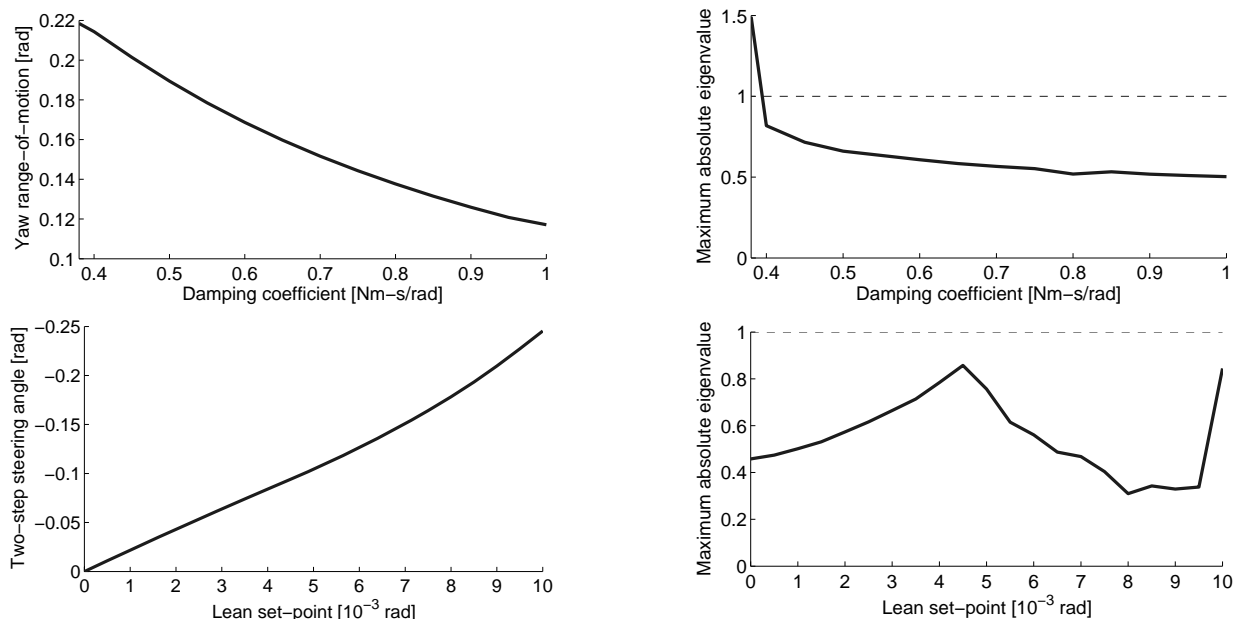

Fig. 3. Top: yaw range-of-motion (left) and maximum eigenvalue modulus (right) of straight-ahead gait against yaw viscosity K_ψ. Bottom: two-step steering angle (left) and maximum eigenvalue modulus (right) of turning gait against lean set-point $\bar{\varphi}_{in}$ of the inner leg.
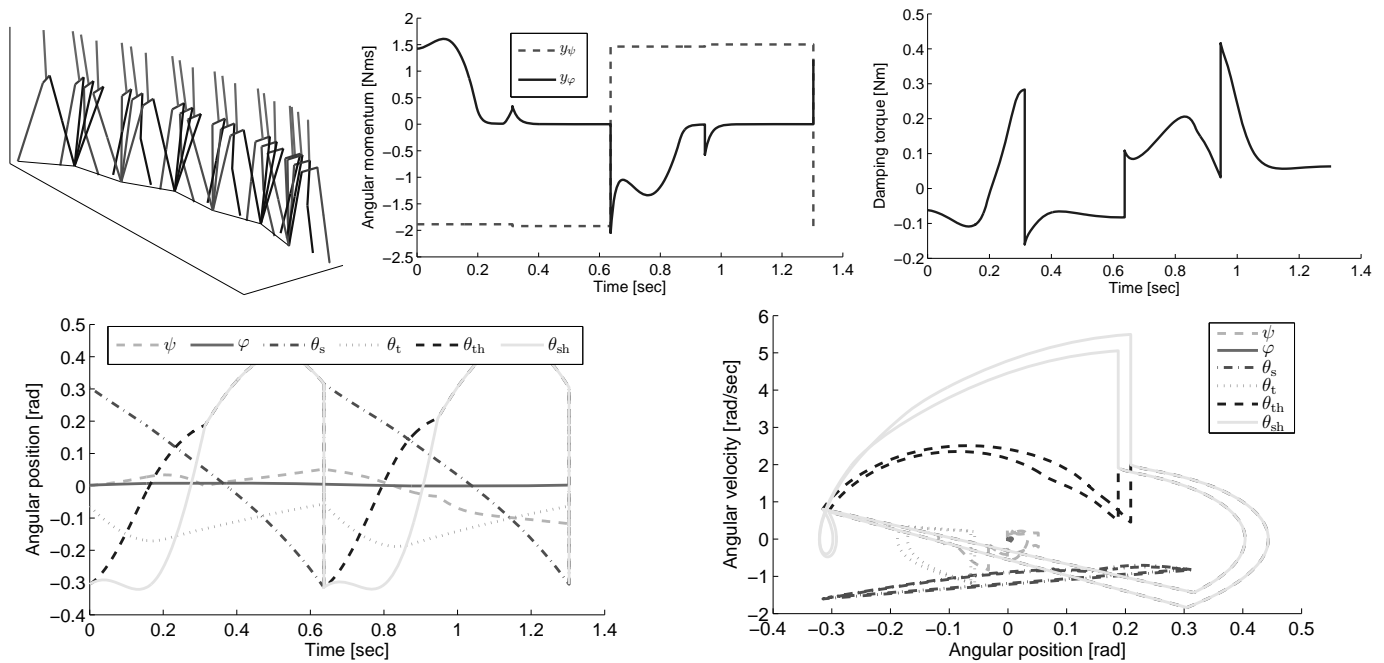
Fig. 4. Steering gait animation (top-left), outputs (top-center), yaw damping torque (top-right), joint trajectories (bottom-left), and phase portrait (bottom-right). A supplemental movie of the steering gait is available at: http://vimeo.com/23020181.

which currently allow more yaw range-of-motion than biological legs [3], could improve gait stability with additional damping. This begs questions about the role of friction dynamics and momentum conservation in human locomotor control, especially for turning strategies that pivot about the stance leg [4], which could inform humanoid robot control strategies.

REFERENCES

[1] J. W. Grizzle, C. Chevallereau, A. D. Ames, and R. W. Sinnet, "3D bipedal robotic walking: Models, feedback control, and open problems," in *IFAC Symp. Nonlin. Control Syst.*, Bologna, Italy, 2010, pp. 505–532.

[2] J. Rose and J. G. Gamble, *Human Walking*, 3rd ed. New York, NY: Lippincott Williams & Wilkins, 2006.

[3] K. Flick, M. Orendurff, J. Berge, A. Segal, and G. Klute, "Comparison of human turning gait with the mechanical performance of lower limb prosthetic transverse rotation adapters," *Prosth. Orth. Int.*, vol. 29, no. 1, p. 73, 2005.

[4] M. Taylor, P. Dabnichki, and S. Strike, "A 3-D biomechanical comparison between turning strategies during the stance phase of walking," *Human Movement Sci.*, vol. 24, no. 4, pp. 558–573, 2005.

[5] M. Twiste and S. Rithalia, "Transverse rotation and longitudinal translation during prosthetic gait–A literature review," *J. Rehab. Res. Dev.*, vol. 40, no. 1, pp. 9–18, 2003.

[6] C. Chevallereau, J. W. Grizzle, and C. L. Shih, "Steering of a 3D bipedal robot with an underactuated ankle," in *IEEE Int. Conf. Intell. Robots Syst.*, Taipei, Taiwan, 2010, pp. 1242–1247.

[7] E. R. Westervelt, J. W. Grizzle, C. Chevallereau, J. H. Choi, and B. Morris, *Feedback Control of Dynamic Bipedal Robot Locomotion*. New York, NY: CRC Press, 2007.

[8] R. D. Gregg and M. W. Spong, "Reduction-based control of three-dimensional bipedal walking robots," *Int. J. Robot. Res.*, vol. 26, no. 6, pp. 680–702, 2010.

[9] ——, "Reduction-based control of branched chains: Application to three-dimensional bipedal torso robots," in *IEEE Conf. Dec. Control*, Shanghai, China, 2009, pp. 8166–8173.

[10] ——, "Bringing the compass-gait bipedal walker to three dimensions," in *IEEE Int. Conf. Intell. Robots Syst.*, St. Louis, MO, 2009, pp. 4469–4474.

[11] R. D. Gregg, L. Righetti, J. Buchli, and S. Schaal, "Constrained accelerations for controlled geometric reduction: Sagittal-plane decoupling in bipedal locomotion," in *IEEE Int. Conf. Human. Robot.*, Nashville, TN, 2010.

[12] M. W. Spong and F. Bullo, "Controlled symmetries and passive walking," *IEEE Trans. Autom. Control*, vol. 50, no. 7, pp. 1025–1031, 2005.

[13] A. D. Ames and R. D. Gregg, "Stably extending two-dimensional bipedal walking to three dimensions," in *Amer. Control Conf.*, New York, NY, 2007, pp. 2848–2854.

[14] R. D. Gregg, A. Tilton, S. Candido, T. Bretl, and M. W. Spong, "Control and planning of 3-D dynamic walking with asymptotically stable gait primitives," *IEEE Trans. Rob.*, vol. 28, no. 6, pp. 1415–1423, 2012.

[15] R. D. Gregg, "Controlled geometric reduction of a five-link 3D biped with unactuated yaw," in *IEEE Conf. Dec. Control*, Orlando, FL, 2011, pp. 669–674.

[16] J. E. Marsden and T. S. Ratiu, *Introduction to Mechanics and Symmetry*, 2nd ed. New York, NY: Springer, 2002.

[17] J. W. Grizzle, C. H. Moog, and C. Chevallereau, "Nonlinear control of mechanical systems with an unactuated cyclic variable," *IEEE Trans. Autom. Control*, vol. 50, no. 5, pp. 559–576, 2005.

[18] R. D. Gregg, "Geometric control and motion planning for three-dimensional bipedal locomotion," Ph.D. dissertation, University of Illinois at Urbana-Champaign, 2010.

[19] D. E. Chang and S. Jeon, "Damping-induced self recovery phenomenon in mechanical systems with an unactuated cyclic variable," *J. Dyn. Syst. Meas. Control*, vol. 135, no. 2, p. 021011, 2013.

[20] R. Sepulchre, M. Janković, and P. V. Kokotović, *Constructive Nonlinear Control*. New York, NY: Springer-Verlag, 1997.

[21] L. Sentis and O. Khatib, "Synthesis of whole-body behaviors through hierarchical control of behavioral primitives," *Int. J. Human. Robot.*, vol. 2, no. 4, pp. 505–518, 2005.

[22] F. Asano and M. Yamakita, "Extended PVFC with variable velocity fields for kneed biped," in *IEEE Int. Conf. Human. Robot.*, 2000.

[23] P. De Leva, "Adjustments to Zatsiorsky-Seluyanov's segment inertia parameters," *J. Biomech.*, vol. 29, no. 9, pp. 1223–1230, 1996.

[24] C. Chevallereau, D. Djoudi, and J. W. Grizzle, "Stable bipedal walking with foot rotation through direct regulation of the zero moment point," *IEEE Trans. Rob.*, vol. 24, no. 2, pp. 390–401, 2008.

[25] S. H. Collins and A. Ruina, "A bipedal walking robot with efficient and human-like gait," in *IEEE Int. Conf. Robot. Autom.*, Barcelona, Spain, 2005, pp. 1983–1988.

[26] K. Sreenath, H. W. Park, I. Poulakakis, and J. W. Grizzle, "A compliant hybrid zero dynamics controller for stable, efficient and fast bipedal walking on MABEL," *Int. J. Robot. Res.*, vol. 30, no. 9, pp. 1170–1193, 2011.